Lawrence Berkeley National Laboratory
Recent Work

Title
TWINS IN HIGH-T[SUB]C YBA[SUB]2 CU[SUB]3 O[SUB]7-DELTA SUPERCONDUCTORS

Permalink
https://escholarship.org/uc/item/7mn3682w

Authors
Jon, C.J.
Mashburn, J.

Publication Date
1988-10-01

eScholarship.org Powered by the California Digital Library
University of California

Center for Advanced Materials

CAM

RECEIVED
LAWRENCE
BERKELEY LABORATORY
JAN 25 1989
LIBRARY AND
DOCUMENTS SECTION

To be published as a chapter in **Studies of High Temperature Superconductors**, A.V. Narlikar, Nova Science Publishers, Inc. Commack, NY

Twins in High-T_c $YBa_2Cu_3O_{7-\delta}$ Superconductors

C.J. Jou and J. Washburn

October 1988

TWO-WEEK LOAN COPY

This is a Library Circulating Copy which may be borrowed for two weeks.

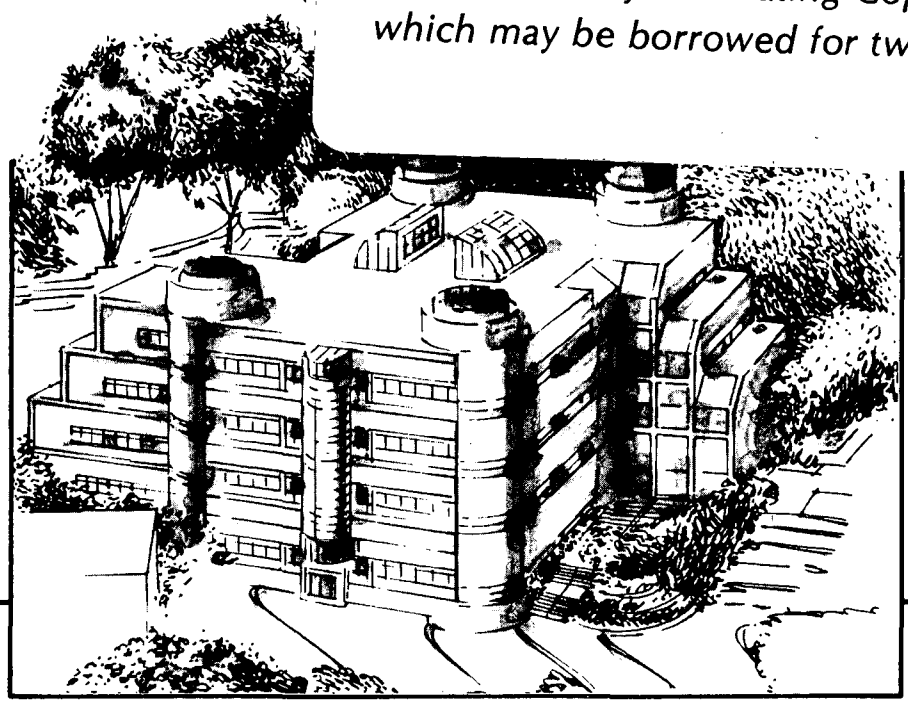

Materials and Chemical Sciences Division

Lawrence Berkeley Laboratory • University of California

ONE CYCLOTRON ROAD, BERKELEY, CA 94720 • (415) 486-4755

Prepared for the U.S. Department of Energy under Contract DE-AC03-76SF00098

LBL-26108

DISCLAIMER

This document was prepared as an account of work sponsored by the United States Government. While this document is believed to contain correct information, neither the United States Government nor any agency thereof, nor the Regents of the University of California, nor any of their employees, makes any warranty, express or implied, or assumes any legal responsibility for the accuracy, completeness, or usefulness of any information, apparatus, product, or process disclosed, or represents that its use would not infringe privately owned rights. Reference herein to any specific commercial product, process, or service by its trade name, trademark, manufacturer, or otherwise, does not necessarily constitute or imply its endorsement, recommendation, or favoring by the United States Government or any agency thereof, or the Regents of the University of California. The views and opinions of authors expressed herein do not necessarily state or reflect those of the United States Government or any agency thereof or the Regents of the University of California.

TWINS IN HIGH-T_c $YBa_2Cu_3O_{7-\delta}$ SUPERCONDUCTORS

C.J. Jou and J. Washburn

Department of Materials Science and Mineral Engineering
University of California
and
Center for Advanced Materials
Materials and Chemical Sciences Division
Lawrence Berkeley Laboratory
1 Cyclotron Road
Berkeley, CA 94720

I. INTRODUCTION

Since discovery of the La-Ba-Cu-O (LBCO) system of high-T_c oxide superconductors with $T_c \sim 28°$ K in 1986 [1], a world-wide search for other oxide superconductors has resulted in the discovery of the Y-Ba-Cu-O (YBCO) system with $T_c \sim 93°$ K in 1987 [2], two new classes in 1988, i.e., the Bi-Ca-Sr-Cu-O (BCS) system [3] and the Tl-Ca-Ba-Cu-O (TCB) systems [4], with the highest reported $T_c \approx 110°$ K and 125° K respectively. Also, a perovskite-related Ba-K-Bi-O (BKBO) system [5] with $T_c \sim 30°$ K became the first known high-T_c oxide superconductor in the bismuth oxide family. The discovery of each class provided a new challenge to the fundamental understanding of superconductivity. For example, the discovery of the YBCO system initiated a race to find a superconducting mechanism related to the oxygen-ordered Cu-O chain structure. When the BCS and TCB systems were discovered, which did not contain the linear chain structure of the YBCO system but had even higher T_c, emphasis shifted to the CuO_2 layers that were common to all the high T_c copper oxide superconductors. All except BKBO share a common pseudo-two-dimensional structure with CuO_2 planes sandwiched between metallic layers. This structure appears to play a critical role for the observed superconductivity. In all of these materials the structure can be described by stacked perovskite-related unit cells. They all show bad metallic properties above T_c and are all oxygen-deficient because of doping with randomly distributed dopants having different charges, e.g., A^{II} in $(La^{III}_{1-x} A^{II}_x)_2 CuO_{4-\delta}$ with A = Ba, Sr or Ca and K^I in $(Ba^{II}_{0.6} K^I_{0.4})BiO_{3-\delta}$. $La^{III}_2 CuO_4$ and $Ba^{II}BiO_3$ are insulators. For the YBCO, BCS and TCB systems, Cu^{III}, Bi^{III} and Tl^{III} can be considered as substitutional dopants in the three-dimensional Cu^{II} lattice which result in randomly distributed oxygen vacancies in the capping layers, i.e., $Cu^{III}O$ in $YBa_2Cu_3O_{7-\delta}$, $Bi^{III}_2O_2$ in BCS and $Tl^{III}_2O_2$ in TCB. The result of this doping is that the uniformity of the oxidation state (III) of cations in the capping layer(s), which is also a common feature in copper oxide superconductors, is destroyed. A defected macro-resonance-cell model [6] has been proposed to qualitatively discuss superconductivity in these oxides. The cations in the capping layers all have in common various oxidation states with charge difference two, e.g., Tl with I and III, Bi with III and V, Pb with II and IV and Cu with I, II and III.

Among all the classes of high-T_c oxide superconductors, the YBCO system has the most unusual features in its structure. The cation in its capping layer, CuO, is the same as that of the CuO_2 layers. Hence, the Cu cations in this structure form a three-dimensional frame similar to the Bi frame in the BKBO system. The stacking sequence of the YBCO system has only a single period and single boundary layer, unlike the other systems, all of which have a double period with phase shift as the stacking sequence is followed through the center of the double boundary layers (see Table I.1). Also, oxygen atoms in the capping layer of the YBCO system are ordered forming a linear chain structure on the basal plane. This oxygen (vacancy) ordering mechanism results in an orthorhombic structure which in turn results in a finely twinned microstructure which is formed when the structure changes from tetragonal to orthorhombic on cooling. However, this oxygen ordering can only take place when the oxygen content, x, in $YBa_2Cu_3O_x$, is larger than about 6.5. For x below 6.5, oxygen atoms on the basal plane are randomly distributed resulting in a tetragonal structure which is nonsuperconducting. For the superconducting orthorhombic structure, the critical temperature, T_c, is strongly dependent on the oxygen content [7], and therefore on the amount and the distribution of the oxygen vacancies. In this chapter, a twin formation mechanism is discussed and an oxygen-depleted twin boundary model is proposed that may explain the observed difficulty of reaching the stoichiometric composition, x = 7, in orthorhombic YBCO.

Table I.1. Stacking sequence of layers in unit cell.

$YBa_2Cu_3O_7$	(n=2)	Ba		O_2	Y	O_2	Ba	O	← center									
									← edge									
		O		Cu		Cu	O	Cu	← corner									
$Bi_2CaSr_2Cu_2O_8$	(n=2)	O	Sr	O_2	Ca	O_2	Sr	O	Bi	O	Cu		Cu	O	Bi			
											O_2		O_2					
		Bi	O	Cu		Cu	O	Bi	O	Sr		Ca		Sr	O			
$Tl_2CaBa_2Cu_2O_8$	(n=2)	O	Ba	O_2	Ca	O_2	Ba	O	Tl	O	Cu		Cu	O	Tl			
											O_2		O_2					
		Tl	O	Cu		Cu	O	Tl	O	Ba		Ca		Ba	O			
La_2CuO_4	(n=1)	O	Cu	O	La		La											
			O_2															
		La		La	O	O_2	O											
		boundary ← → layer(s)																

II. FORMATION OF COHERENT TWINS IN $YBa_2Cu_3O_{7-\delta}$ SUPERCONDUCTORS

The 1-2-3 structure of the $YBa_2Cu_3O_x$ system, $6 \leq x \leq 7$, has a unique property—the so called "oxygen sponge," i.e., when cooling from the sintering temperature, T_s, usually around 950°C, oxygen content increases monotonically (Fig. 1a) and when heating up, oxygen content decreases. The oxygen disorder-order induced phase transition from the semiconducting tetragonal structure to the superconducting orthorhombic structure is accompanied by the formation of coherent twins at

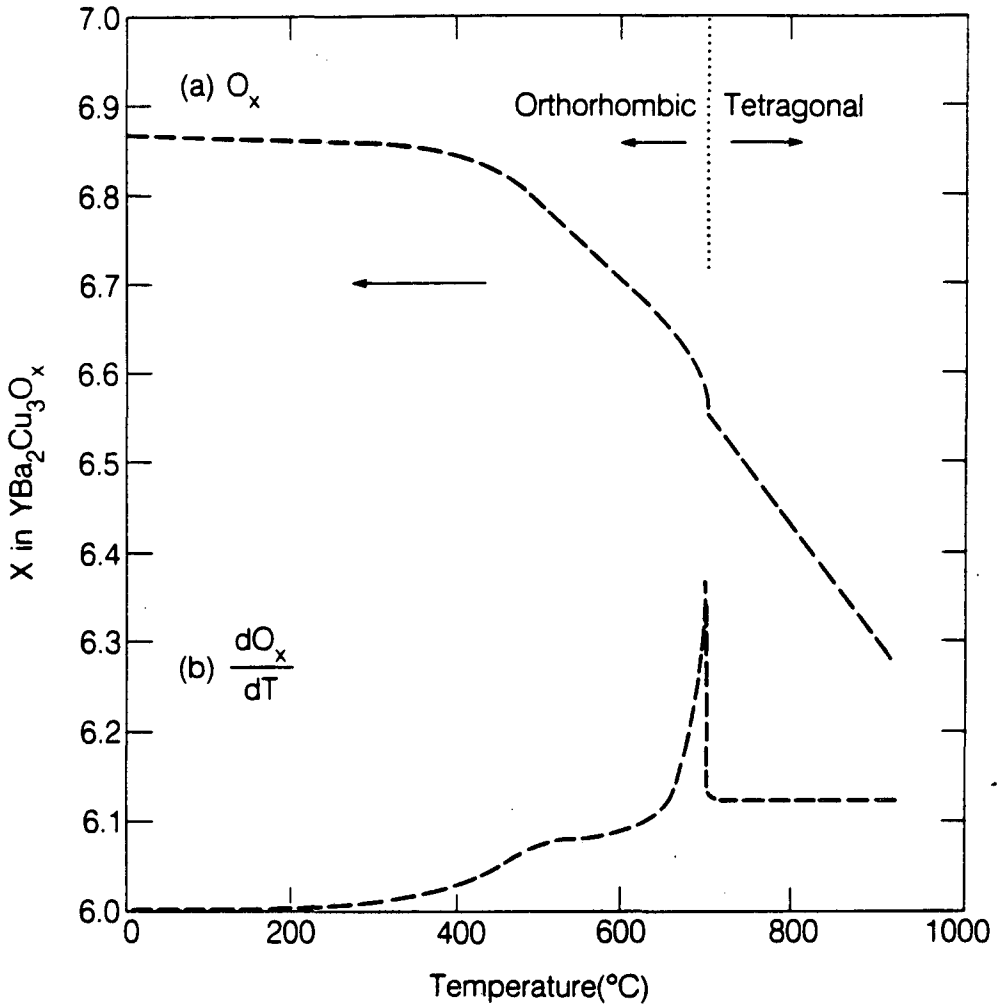

Fig. 1. (a) Total oxygen content, x, in $YBa_2Cu_3O_x$ increases monotonically when cooled slowly from sintering temperature in 1 atm O_2 ambient. Note there is a kink at the structure transition temperature T_p. Data deduced from Ref. 1. Scale of O_x is for (a) only. (b) The differentiation of the curve in (a) reveals a peak at T_p forming the characteristic "λ" curve of a second order phase transformation. Oxygen ordering on the basal plane is in progress starting at T_p.

temperature T_p and oxygen content $(O_x)_p$. Below T_p, the structure is orthorhombic with oxygen content $O_x > (O_x)_p$ when cooled slowly in an oxygen-rich ambient from the sintering temperature, T_s. Above T_p, the structure is tetragonal with $O_x < (O_x)_p$. The rate of oxygen uptake increases sharply at T_p as shown in Fig. 1b which has the characteristic "λ" shape of a second order phase transition. Below 650°C it drops back to about the same rate as just before T_p, and with further cooling decreases gradually until by about 300°C no further oxygen uptake occurs. Both T_p and $(O_x)_p$ are a function of the oxygen partial pressure, P_{O_2}, in the ambient under equilibrium conditions, e.g., for P_{O_2} = 1 atm (in 100% pure oxygen ambient), $T_p \approx 700$°C, for P_{O_2} = 0.2 atm (in air or 20% O_2–80% Ar ambient), $T_p \approx 670$°C, and for $P_{O_2} \approx 0.02$ atm (in vacuum or 2% O_2–98% Ar), $T_p \approx 620$°C, and $(O_x)_p$ in this partial pressure range is about 6.5 ~ 6.6 [8]; when P_{O_2} decreases both T_p and $(O_x)_p$ decrease.

Based on this information and in-situ transmission electron microscope (TEM) observations [9-12], a model describing the mechanism of formation of coherent twins is presented which can help to explain some of the observed experimental results. In the slow cooling step, which is essential for good quality high T_c material, the cooling rate, dT/dt, is small and usually constant. The changing oxygen content dO_x/dt can thus also be considered as dO_x/dT. Although the diffusivity of oxygen in the material also changes as temperature decreases, for slow cooling rates and in not too low a temperature range it can be assumed that equilibrium is approached at least in porous or thin specimens. As seen in Fig. 1b, $dO_x/dT \simeq dO_x/dt$ is the order parameter for this phase transition.

1. Nucleation

As revealed by in-situ neutron powder diffraction [8], at temperature just above T_p, i.e., the tetragonal structure, O(4) and O(5) sites are randomly occupied by equal amounts of oxygen with an average occupancy of each site about 1/4. The O(1) sites on the BaO layer, O(2) and O(3) sites on the CuO_2 layer are all fully occupied. At T_p the occupancy of the (0, 1/2, 0), O(4), b-chain sites on the CuO basal plane layer, starts increasing at a faster rate than the decrease of occupancy on the (1/2, 0, 0), O(5), sites on the same layer. This suggests that the increased uptake of oxygen from the ambient goes primarily to the b-chain sites and an oxygen ordering process is in progress. The overall oxygen content increases at a rate much larger than just above T_p (Fig. 1b) indicating incorporation of oxygen from the ambient into the material is facilitated by the structural transformation. It is suggested here that this sudden increase of oxygen absorption rate is associated with a nucleation process, the formation of embryos of the orthorhombic phase.

Since the oxygen-ordered orthorhombic phase contains the linear chain structure on the basal plane, these embryos are assumed to consist of clusters of short parallel b-chains, i.e., Cu(1)-O(4)-Cu(1). They should first appear at the heterogeneous sites located at grain surfaces, i.e., grain boundaries and pore surfaces, since the internal stress due to the localized distortion associated with b-chain growth in the tetragonal matrix can be at least partially relaxed (Fig. 2). The formation of b-chain embryos at grain boundaries probably first develops by consuming oxygen in the O(4)-O(5) basal plane which would soon become depleted near the grain boundaries. Further growth of the orthorhombic ordered phase then would require a supply of oxygen from the ambient through the pore-grain boundary network (Fig. 2). Clusters of b-chains with b directions orthogonal to each other are equally probable because of the symmetry of the parent tetragonal structure. Furthermore, for stress compensation nucleation of an embryo with one b-chain direction tends to induce the nucleation of another with an orthogonal b-chain direction. Below T_p the oxygen-ordered configuration on O(4)-O(5) basal plane has a lower free energy than that of the oxygen-disordered configuration [13]. Once initiated at a grain surface the extension of b-chains should be rapid. An elongated embryo with an oxygen-depleted zone around it is expected.

In powder-sintered materials, depending on the pressing process and the sizes and kinds of powders, there are many voids and open channels among grains. For high porosity material, the total internal pore surface area may be larger than the total area of the grain boundaries. This free surface area may play a significant role in determining the physical properties of such a material. Grain boundaries also permit faster diffusion than that possible through a grain because of the looser structure. Significant diffusion of oxygen within a grain along the c-axis direction is unlikely to happen at temperatures below T_p. Oxygen from the environment and from pore surfaces is likely to be distributed to the grains deep inside the sample primarily through this pore-grain boundary network. To diffuse into the grain, oxygen probably has to find a basal plane edge. Hence, grain boundary diffusion would often be required for supplying oxygen from the ambient to parts of the grains.

As b-chain clusters at grain boundaries grow, embryos probably also develop homogeneously or heterogeneously inside the grain by local oxygen ordering. They are probably formed somewhat later than those at grain surfaces, since the internal stress developed by the b-chain ordering can not be partially relaxed as at grain surfaces and the incorporation of the limited available oxygen is

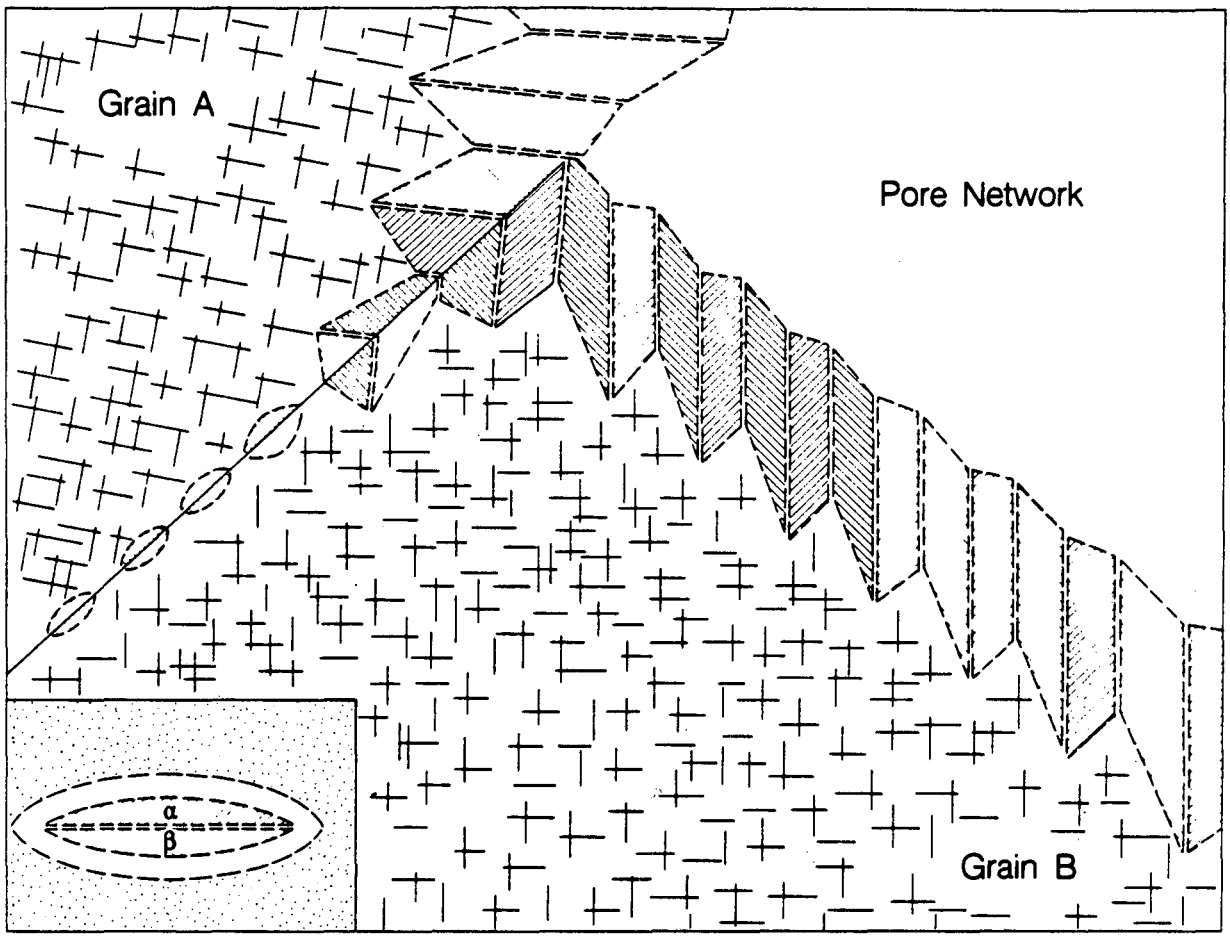

Fig. 2. Proposed nucleation of ordered oxygen clusters starts at grain surfaces, i.e., grain boundaries or pore surfaces, where the stress due to structural transformation can be partially relaxed. When two neighboring clusters with orthogonal b-chain directions meet, coherent twin boundaries with an oxygen-depleted zone are formed. Twin nuclei (insert at lower left corner) are formed later in the interior of the grain. They consume most of the available oxygen content in the grain at T_p forming a heavily interpenetrated tweed structure (Fig. 3a). An oxygen concentration gradient between the grain surface and the grain interior is set up. Further growth of the twin laths in the grain is limited by diffusion of oxygen into the grain center. The twin nuclei at the grain surfaces can grow faster with the oxygen supplied directly from ambient via the pore-grain boundary network and the oxygen-depleted twin boundaries. During the growth, twin laths in the grain interior are incorporated at the growth front.

competitive among embryos in the central region of the grain. The available oxygen would be quickly consumed by the formation of such nuclei. Oxygen-depleted zones would be formed around these nuclei setting up a concentration gradient between center and surface of the grains, causing more oxygen to diffuse into the grain. These b-chain clusters have locally the orthorhombic lattice structure with the lattice constants, a and b on the basal plane, smaller and larger, respectively, than a_t of the parent tetragonal lattice. The tetragonal matrix surrounding the elongated nucleus experiences contraction at the ends of the b-chains and expansion at the sides parallel to the b-chains. When two clusters with orthogonal b-chain directions approach each other, the oxygen depleted zones and the strain fields overlap causing a reduction of the stress along one <110> direc-

tion and enhancement along the orthogonal <110> direction; impingement of the two domains along the latter <110> direction eventually results in formation of a coherent twin boundary. The equilibrium width of the twin boundary zone is assumed in this model to be determined by a balance between the coulomb repulsion force of oxygen ions at opposite sides of the boundary and the chemical potential favoring extension of the b-chains. A "twin nucleus" within the grain with a narrow oxygen-depleted zone remaining at the twin boundary is expected (Fig. 2, left lower corner).

Either <110> direction on the basal plane can lie parallel to a twin boundary, i.e., the twin nuclei have two equally probable twin boundary orientations perpendicular to one another. These nuclei have been observed by in-situ TEM as randomly distributed and inter-penetrated orthogonal sets, a tweed-like structure (Fig. 3) [14-16]. Other combinations of b-chain nuclei, quartet, etc., are also possible, but with smaller probability than doublet. When two b-chain clusters with the same b-chain direction approach each other, coalescence takes place resulting in a larger b-chain cluster.

Since oxygen content (O_{x_p}) is about 6.5 at T_p, only half of the available b-chain sites of the orthorhombic phase in the grain are occupied by oxygen, i.e., the total volume of the orthorhombic twin nuclei is only about half the total volume of the grain. This leaves a relatively open structure for oxygen diffusion. Further transformation requires oxygen diffusion into the grain, the driving force being the tendency for further extension of b-chains, resulting in the observed sudden rise in rate of oxygen uptake at T_p as shown in Fig. 1b.

2. Growth

The b-chain clusters nucleated at grain surfaces grow most rapidly by incorporating oxygen readily supplied from the ambient. When the transformation is complete at grain surfaces, the diffusion of oxygen into the grain becomes more restricted, i.e., oxygen-depleted twin boundary zones.

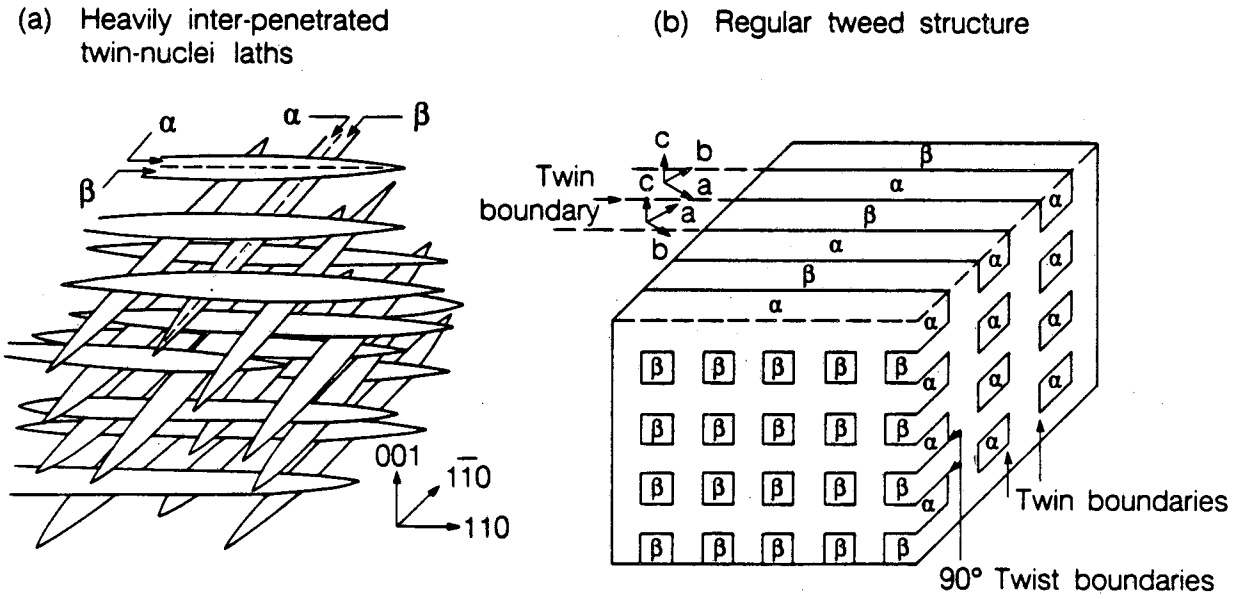

Fig. 3. (a) Interpenetrated twin laths leave the untransformed matrix oxygen-depleted inside the grain. (b) A fully grown tweed structure would form a two-dimensional mutually-modulated regular pattern, possibly observed in some in-situ transmission electron microscopy observations during cooling from high temperature. The electron diffraction pattern of this structure may reveal an effective unit cell with $\sqrt{2}a \times \sqrt{2}a \times \sim 3a$. However, the structure contains both twin boundaries and high energy 90°-rotation boundaries, therefore it would be a metastable intermediate product.

This can explain the sharp decrease of the rate of oxygen uptake below T_p (see Fig. 1b). The growth front of the twinned orthorhombic structure nucleated at grain surfaces gradually extends deeper into the grain by adding new b chains at the growth front with oxygen being supplied from ambient via the pore-grain boundary twin boundray network and by incorporating twin nuclei that have already formed inside the grain.

3. Coarsening

During the last stage of twin formation, coarsening takes place eliminating some of the twin boundaries, and thus decreasing total free energy. Small domains included within larger domains tend to disappear by localized oxygen diffusion within the boundary. As long as the temperature is still high enough to permit oxygen diffusion, this climbing process continues to coarsen the twin domains until the widths of the twins are several hundred Å. Rapid cooling severely inhibits this coarsening process; the resulting structure contains more numerous fine twins. When cooling rate is very rapid, e.g., quenching from temperature above T_p, the tetragonal structure is partially preserved with oxygen content less than 6.5. There is insufficient time for oxygen absorption and thus insufficient oxygen to complete the growth of the b-chain orthorhombic structure. Quenching from temperature between ~350°C and T_p yields intermediate T_c with oxygen contents between 6.8 and 6.6. Sintered polycrystalline $YBa_2Cu_3O_{7-\delta}$ is usually given a low temperature annealing step to enhance its superconducting properties. The annealing temperature is typically chosen below T_p but above 400°C in an oxygen-rich environment to permit further coarsening, stress relaxation and oxygen uptake.

III. MODELS AND SIMULATIONS OF OXYGEN-DEPLETED TWIN BOUNDARIES

1. Models

A model of twin boundaries in orthorhombic $YBa_2Cu_3O_x$ superconductors with a number of layers (j) containing oxygen vacancies at twin boundaries [17] (Fig. 4) avoids bringing oxygen neighbors too close together while preserving coherency at twin boundaries. The oxygen-depleted

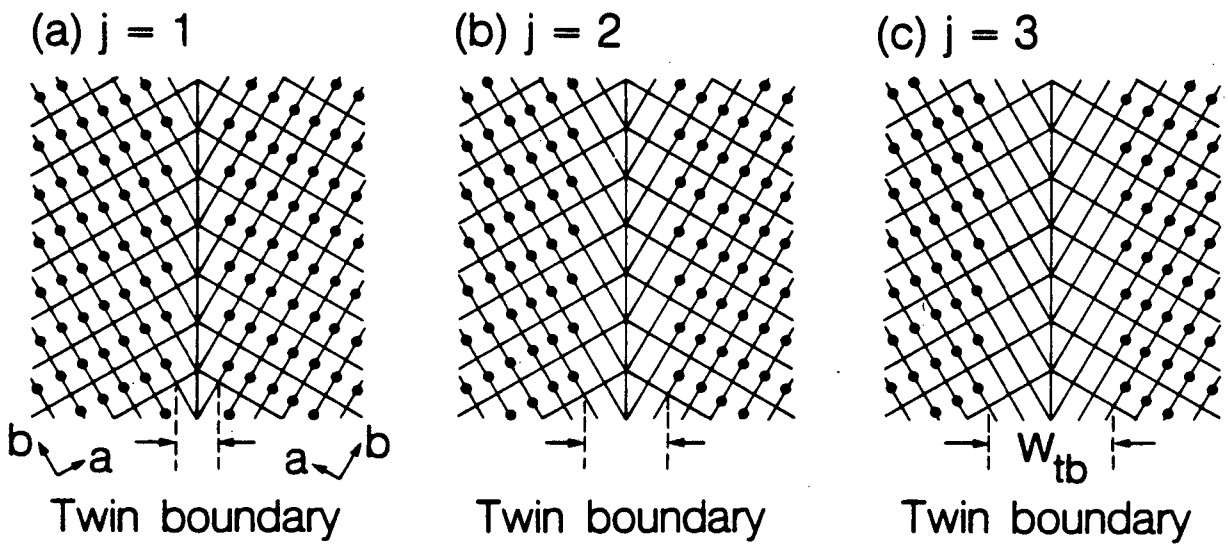

Fig. 4. Oxygen vacant twin boundary models for (a) 1 vacant layer (j=1), (b) 3 vacant layers (j=2), and (c) 5 vacant layers (j=3). Note: The angle at twin boundaries and the length difference between the lattice constants (a) and (b) are exaggerated. For simplicity, only oxygen atoms (black dots) are shown.

twin boundary width can be expressed as $W_{tb}(j) = 2j\ ab/(a^2 + b^2)^{1/2}$. Taking the estimated average twin width [18] as: $W_t \simeq ab/(b - a)$ and assuming a perfect stoichiometric $YBa_2Cu_3O_7$ within the twin domains and $YBa_2Cu_3O_6$ at twin boundaries, then the average oxygen content, x, in $YBa_2Cu_3O_x$, which would be experimentally measured, is:

$$x(j) = 6 + \frac{W_t - W_{tb}(j)}{W_t} = 7 - \frac{W_{tb}(j)}{W_t} = 7 - \frac{2j\,(b-a)}{\sqrt{a^2 + b^2}} \quad .$$

Applying a = 3.822 Å, b = 3.891 Å from the work of Cava et al. [7], the calculated values of x(j) match the experimentally measured oxygen content very well (Table III.1) suggesting that in their samples, near perfect stoichiometric $YBa_2Cu_3O_7$ may form within the twin domains but a few layers of oxygen depletion exist at twin boundaries. The oxygen deficiency study [22] seems to indicate that under normal pressure processing, i.e., 1 atm O_2 or air, the ultimate oxygen stoichiometry is about 6.93 or equivalent to the case j = 3. However, there must always be some vacancies dispersed within the twin domains at random or in an ordered structure [29]. Thus the number of oxygen vacant layers at twin boundaries may be smaller than that calculated.

Table III.1

j	1	2	3	4	5	6	7	8	9
x(j)	6.975	6.949	6.924	6.899	6.873	6.848	6.823	6.798	6.772
x_{exp}	6.975[7] 6.97[19]	6.94	6.92 ± 0.01[21] 6.92[19,22]	(~6.9)	6.87	6.85	6.82	6.80	6.78
Ref.	7,19	20	19,21,22	23	24	25–27	28	19,26	7
T_c(°K)	90[7]	89	95[22]	87	90	91[25]	91	NA	83

2. Simulations

Simulated high resolution electron microscope (HREM) images of twin boundaries with various j values, different defocussing conditions and different sample thicknesses are shown in Fig. 5a-c respectively. The simulated images of the twin boundaries assuming no oxygen vacancies [(Fig. 5a) top] show no contrast across the twin boundaries regardless of the objective lens defocus and sample thickness. However, when a few layers of oxygen at twin boundaries are taken away, contrast across twin boundaries appears. The width of the contrast band increases in proportion to j as shown in Fig. 5a. Contrast at the twin boundaries also varies markedly with defocussing conditions as shown in Fig. 5b. Note that the apparent boundary widths also vary slightly. Contrast at twin boundaries due to sample thickness variation, as shown in Fig. 5c, is equally dramatic. It can vary from almost no contrast to strong contrast. Various band widths and different contrast at twin boundaries in real HREM images are commonly observed [14,30-32] in agreement with the model proposed here (Fig. 6). Also, twin boundaries exposed to a focussed beam for a short time, e.g., 1 minute, show a decrease in contrast [10]. Oxygen atoms in twin domains close to the twin boundaries may gain energy through electron bombardment to jump into the twin boundary vacancies. Thus, the contrast might be expected to smear out as illustrated by the simulated images in Fig. 5d.

3. Discussion

A study by Chen et al. [16] shows that the ordered vacancies within the body of the twin domains accounts for only 3% of the total volume in a $YBa_2Cu_3O_{6.72}$ sample. This discrepancy

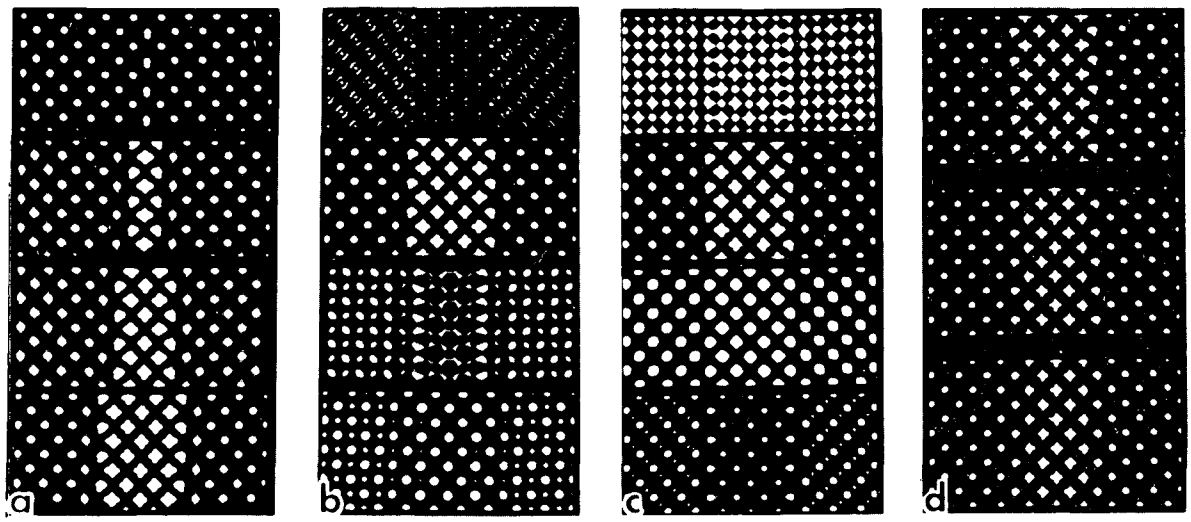

Fig. 5. Simulated HREM [001] images of twin boundaries. Simulation parameters are chosen to correspond to the operating conditions in the JEOL 4000 FX electron microscope. Sample thickness is 100Å and objective lens defocus is –800Å unless specified otherwise. (a) Changes with respect to j from j = 0 (no oxygen depleted layer, top) to j = 3 (bottom). (b) Variation with respect to objective lens defocus; –400Å (top) to –1600Å (bottom) in increments of –400Å, j = 3. (c) Variation with respect to sample thickness; 50Å (top) to 200Å (bottom) in increments of 50Å, j = 3. (d) Total oxygen atom number fixed, but abrupt concentration changes at twin boundaries are gradually relaxed (j = 3).

could be explained by the oxygen-depleted twin boundary model with $j \approx 3$. The high resolution image shown in Fig. 6 also matches the simulated images using the model proposed here with $j \approx 3$.

Since the equilibrium width of the oxygen-depleted zone at a twin boundary is determined by the balance of the Coulomb repulsion force and the chemical potential, the resulting optimized configuration may have at least one layer of oxygen vacancies condensed at the twin boundary (j = 1 case) where the repulsion energy is the highest. For $j \geq 2$, the repulsion energy decreases inversely proportional to the oxygen ion distance resulting in increasingly diffuse oxygen-depleted layers, i.e., oxygen-vacancy segregation at these layers is probably incomplete. For simplicity, however, this diffuse atmosphere of oxygen vacancies has been described as a number of layers of oxygen vacancies, j.

IV. EFFECTS OF OXYGEN-DEPLETED TWIN BOUNDARIES ON SUPERCONDUCTING PROPERTIES

A defected macro-resonance-cell (MRC) model for high-T_c oxide superconductors [6] based on their common features and minimum energy principles suggests that copper in its high oxidation state may dissociate into the fundamental, i.e., the lowest, oxidation state and contribute hole(s) as charge carriers. In the normal conducting (NC) state of $YBa_2Cu_3O_7$, each Cu on the CuO basal plane contributes two holes ($Cu^{+3} \rightarrow Cu^{+1} + 2h$) for conduction and Cu on the CuO_2 planes contributes one hole ($Cu^{+2} \rightarrow Cu^{+1} + h$). In the MRC model, these holes form charge carrier pairs and are delocalized. However, the coupling between CuO and CuO_2 layers is weak in the NC state and the propagation directions of the holes are random except in the presence of an applied field. In the superconducting (SC) state, the oxidation states of copper may oscillate between I and III forming a

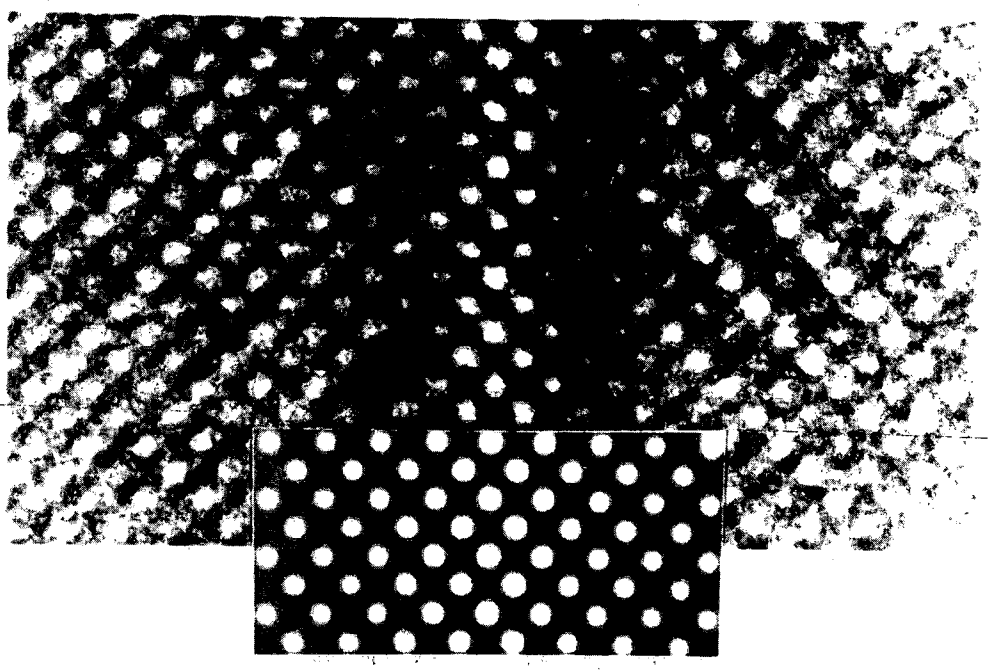

Fig. 6. High resolution electron micrograph of a twin boundary in $YBa_2Cu_3O_x$ material reveals significant contrast across the twin boundary. (Photo courtesy of Dr. K. Hiraga.) Simulated image of an oxygen-depleted twin boundary using model proposed here with j = 3.

three-dimensional resonating network and the coupling between CuO and CuO_2 layers is strong. Free pairs of holes could condense into coherent superconducting pairs. In the static SC mode, i.e., no field applied, there is no net current. In the dynamic SC mode, hole pairs would be driven by the applied field resulting in a net current. In order to permit hole pairs propagation, absence of some holes on the CuO plane, yielding imperfect resonance locally, is essential. This may be realized in several ways, e.g., a small number of O4 jumping to O5 sites, residual oxygen vacancies located on O4 site, doping with elements with different charges, etc. All these defects can cause unsynchronized resonance locally delocalizing hole pairs and shifting the nonconducting (insulating) state into the conducting state. One type of site where oxygen is expected to be deficient is at the twin boundaries if oxygen is depleted on the CuO layer. The CuO_2 layers, on the other hand, already have empty overlapped-orbitals (Cu : $3d_{x^2-y^2}$ and O : 2p) since $Cu^{+2} \rightarrow Cu^{+1} + h$ contributes only one hole. CuO_2 layers must be coupled to the CuO layer to maintain a macro resonance state of the whole lattice.

1. SIS Josephson Junction and Glassy States

Oxygen-depleted twin boundaries with stoichiometric $YBa_2Cu_3O_6$ have CuO_2 planes but are missing the Cu-O chains. Cu at the twin boundaries is in the fundamental oxidation state, Cu^I. Thus the resonance of the Cu frame would not propagate across the twin boundaries, i.e., these twin boundaries are in a nonsuperconducting state. Insulating twin boundaries together with the twin domains on both sides form a superconductor-insulator-superconductor (SIS) Josephson junction. (A similar situation exists at the grain boundaries.) Inside a grain or crystal, the (110) and/or (1 −1 0) twin boundaries together with the (001) 90°-rotation boundaries or grain boundaries would form a three dimensional network dividing the grain into many superconducting clusters weakly

coupled by SIS Josephson junctions. Such a superconducting glassy state including intra- and inter-grain Josephson junctions, would be expected to result in a significant reduction of average current density in polycrystalline oxide superconductors especially when temperature is near T_c [33].

For tunneling to occur, the thickness (d) of the insulating layer, i.e., the width (W_{tb}) of the oxygen-depleted zone at twin boundary or grain boundary, should be smaller than or at most near the coherence length of the oxide superconductor. Since $\xi_{\perp c} \approx 34$ Å [34] ($\xi_{\perp c}$ (77 K) ≈ 60.7 Å [35] or about 42.9 Å across twin boundary), the largest distance the superconducting current could tunnel through at liquid nitrogen temperature would be about eight layers (~ 43.6 Å) of insulating $YBa_2Cu_3O_6$. Experimentally, this expectation is supported by comparing various numbers (j) of oxygen-depleted layers at twin boundary to the J_c (O_x) data [36] (Fig. 7). J_c drops almost linearly with increasing thickness of the insulating layers and approaches zero when $O_x < 6.80$. This is consistent with Cava's [7] measurement of T_c as a function of O_x. In their study, T_c was almost constant for $O_x > 6.80$ and drops quickly when $O_x < 6.78$. For $O_x \approx 6.72$, patches of double cell structure [16,29] with stoichiometric $O_x \approx 6.50$ (homologous phase: 1/2 case) and other homologous phases, e.g., stoichiometric $O_x \approx 6.60$ (homologous phase: 3/5 case) [16], have been found with transmission electron microscopy in the oxygen-heavily-depleted material. In these materials, oxygen vacancies at (0, ½, 0) sites in twin domains and at twin boundaries are reorganized into more stable homologous phases [37], especially the double cell structure [13], with smaller numbers (~ 3) of oxygen-depleted layers at twin boundaries [6,38] which is believed to be the range over which Coulomb repulsion dominates. Presumably, this is also the cause of the peculiar behavior of resistivity in normal conduction [7].

2. Flux Pinning and Vortex State

When a magnetic field is applied to a YBCO superconductor, the nonsuperconducting areas, i.e., twin boundaries as well as grain boundaries with stoichiometric $YBa_2Cu_3O_6$, are expected to

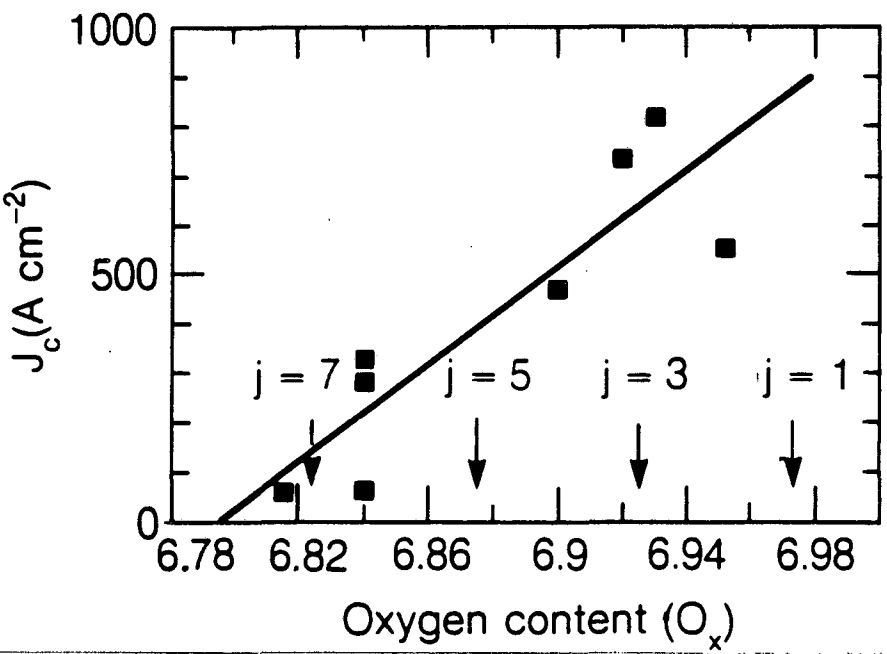

Fig. 7. Critical current density as a function of oxygen content, x, in $YBa_2Cu_3O_x$. Arrows are added to mark the oxygen content of the samples assuming x = 7 within twin domains and various numbers (j) of oxygen depleted layers at twin boundaries. Within these layers x is assumed to be 6. (Reprinted by permission from *Nature* Vol. 332 pp. 58. Copyright (c) 1988 Macmillan Magazines Ltd.)

provide the permeable local paths for magnetic flux lines. That these boundaries act as the pinning sites for flux lines has been successfully demonstrated by the decoration technique [39,40]. Because of the very fine twinning structure, numerous grain boundaries and voids, small grain size and high porosity, as well as the existence of other nonsuperconducting phases, e.g., CuO, $BaCuO_2$ and Y_2BaCuO_5, a regular flux lattice in the vortex state is difficult to obtain. Near liquid nitrogen temperature, only partial flux lattices have been observed [39]. Also, in YBCO material, because the average width of the twin domains, $w_{td} \approx 200 - 300$ Å, is smaller than the penetration distance, $\lambda_{\parallel c} \approx 1250$ Å [34], a regular flux lattice with all lattice sites pinned at the twin boundaries is unlikely since the vortex diameter is about 2λ [41]. However, the numerous twin boundaries acting as flux pinning sites should raise the lower critical field, H_{c_1}, above the intrinsic value of pure $YBa_2Cu_3O_7$ without twin boundaries.

It is well known that type-II superconductors have a negative surface energy between the normal conducting phase (NCP) and the superconducting phase (SCP). The "glassy" state due to the high density of twin boundaries thus provides a large favorable surface area for SCP nucleation when NCP is cooled from above T_c in zero field or when the field is reduced from above H_{c3} at $T < T_c$. The resulting H_{c2} is therefore expected to be smaller than the intrinsic value for a perfect $YBa_2Cu_3O_7$ domain.

The remanent magnetic moment in the hysteresis loop from the magnetization measurement can be attributed to the trapping of flux lines at these insulating boundaries as well. In addition, the flux pinned at twin boundaries can also explain the less than 100% Meissner effect or imperfect diamagnetism measured in field cooled (FC) YBCO crystals (without grain boundary) in which twin boundaries are the only strong pinning sites when flux exclusion progresses as temperature drops below T_c. In zero field cooled (ZFC) specimens, time-dependent magnetization-relaxation phenomena have been reported by several groups [42-44]. This could be due to the weak linking, i.e., the insulating boundaries, in this material. A stable magnetization configuration (state), which minimizes the energy of all the weak couplings, may not initially be achieved. As time passes, the system may transit from one metastable state to another metastable state having lower energy.

3. Superlattice, Band-folding and Minigaps

When calculating the energy band structure of $YBa_2Cu_3O_{7-\delta}$, a homogeneous matrix extending infinitely in all directions is presumed to exist. In the real material, however, dense twin structure with estimated spacing ~ 216 Å between coherent twin boundaries is almost uniformly present everywhere. Their presence breaks the inversion symmetry of the presumed infinite matrix, introduces boundary mirror and glide symmetry operations into the crystal symmetry, and forms polarized boundaries [45]. Since CuO_2 layers are not strongly affected by the presence of these oxygen-depleted twin boundaries, only energy bands related to the CuO b-chain plane are affected by the new symmetry operation.

Along the direction perpendicular to the twin boundary plane, the whole lattice is similar to a structure with a widely spaced superlattice, i.e., b-chains run zig-zag across twin boundaries with a repeating unit of about 156 b-chain units ($W_t \approx 216$ Å). This superlattice structure with glide symmetry thus requires the b-chain related bands folded into a $\pi/156$ b Brillouin zone in $\vec{k}_y$ direction yielding band degeneracy at zone boundary (Y) and subtle changes toward Γ-point. However, the CuO plane is coupled to the neighboring CuO_2 layers via Peierl's deformation of oxygen atoms creating a Jahn-Teller gap. A calculation employing a tight binding model with 75 b-chain unit [45] reveals minigaps at Y-point with scale as small as 200 kelvin as expected, and unknown gaps at Γ-point. These minigaps give rise to the semiconducting or semimetallic character of the CuO b-chain plane. Due to the splitting of degenerated points at zone boundaries, these densely packed, b-chain-plane-related bands are further flattened. However, T_c should be only slightly enhanced by the twinning geometry.

For an oxygen-depleted $YBa_2Cu_3O_x$ sample with $O_x \geq 6.80$, T_c is almost unchanged since the extrapolation length of the pair potential is about 37 Å [33]. The width of the oxygen depleted region at a twin boundary would never be expected to be this large. For $O_x < 6.78$, the oxygen vacancies dispersed in the twin domains start rearranging into a series of homologous phases with the double cell structure as the most stable end phase in the series and T_c drops rapidly to that of the secondary stable structure (~60° K).

V. CONCLUSION

In conclusion, we have proposed a qualitative description for the formation of the twinned structure in $YBa_2Cu_3O_{7-\delta}$. This model assumes oxygen-depleted twin boundary zones which serve as the primary oxygen diffusion paths from grain surfaces toward the interior of the grains and thus control the growth rate of the twins in the grain centers. These twin boundaries are formed during the growth of the b-chain embryos which are first nucleated heterogeneously at grain surfaces. The width of the oxygen-depleted twin boundary zones should be determined by the balance of the chemical potential energy at the ends of the b-chains at the edges of the twin domains and the coulomb repulsion energy between oxygen ions on the opposite sides of the twin boundaries. Under the ordinary processing condition, this is equivalent to the case $j = 3$ in this model. The rapid rate increase of oxygen uptake at T_p is attributed to a high oxygen vacancy concentration in the grain during early stages of the tetragonal to orthorhombic transformation caused by the formation of embryos which quickly consume a large fraction of the oxygen in the grain at T_p. Completion of the transformation by growth of twins occurs most rapidly at the grain surfaces by absorbing oxygen from the ambient and more slowly in grain interiors. Coarsening of the twin domains then occurs by elimination of small domains included within larger domains by localized transfer of oxygen atoms across the twin boundaries. This coarsening process takes place during annealing, resulting in residual stress relaxation and reduction of residual oxygen vacancies within the twin domains. The observed oxygen deficiency remaining after long time annealing in oxygen can be explained if it is assumed that the equilibrium structure of coherent twin boundaries contains one or more layers of oxygen vacancies as proposed in this model.

These twin boundaries together with the 90°-rotation boundaries and grain boundaries divide the material into many superconducting clusters weakly coupled by SIS Josephson junctions, i.e., in a superconducting glassy state. Oxygen-depleted twin boundaries may provide hole-absent sites necessary for yielding local imperfect resonance and delocalization of hole pairs. The critical current as expected from the model would decrease as the number of the oxygen-depleted layers increases causing a wider insulating thickness in the SIS Josephson junction structure. The same effect also would be reflected in the room-temperature resistivity which increases almost linearly with increasing numbers ($1 \leq j \leq 3$) of oxygen-depleted layers at twin boundaries. Imperfect Meissner effect, remanent magnetization as well as the time-dependent magnetization-relaxation phenomena all can be qualitatively understood based on this model. Oxygen-depleted twin boundaries can provide not only the pinning sites for the magnetic flux but also the nucleation sites for the superconducting phase, yielding the measured H_{c1} and H_{c2} higher and lower than the intrinsic value respectively. Finally, the model is consistent with the fact that T_c is nearly constant for oxygen contents above 6.8 but drops quickly when oxygen content is less than 6.78 as oxygen vacancies become rearranged into a more stable secondary structure. Even though the model is only qualitative, it is consistent with a large number of experimental observations and may be helpful in further development of a fundamental understanding of superconductivity in this interesting material.

ACKNOWLEDGMENTS

The authors would like to thank Dr. K. Hiraga for sending the high resolution transmission electron micrograph of a twin boundary.

This work was supported by the Director, Office of Energy Research, Office of Basic Energy Sciences, Materials Sciences Division of the U.S. Department of Energy under Contract No. DE-AC03-76SF00098.

REFERENCES

[1] J.G. Bednorz and K.A. Müller, Z. Phys. B 64, (1986) 189.

[2] M.K. Wu, J.R. Ashburn, C.J. Torng, P.H. Hor, R.L. Meng, L. Gao, Z.L. Huang, X.Q. Wang, and C.W. Chu, Phys. Rev. Lett. 58, (1987) 908.

[3] H. Maeda, Y. Tanaka, M. Fukutomi, and T. Asano, Jpn. J. Appl. Phys. 27, (1988) L209.

[4] Z.Z. Sheng and A.M. Hermann, Nature 332, (1988) 138.

[5] L.F. Mattheiss, E.M. Gyorgy, and D.W. Johnson, Jr., Phys. Rev. B 37, (1988) 3745.
R.J. Cava, et al., Nature 332, (1988) 814.

[6] C.J. Jou and T. Washburn, Lawrence Berkeley Laboratory report, LBL-26078.

[7] R.J. Cava, B. Batlogg, C.H. Chen, E.A. Rietman, S.M. Zahurak, and D.J. Werder, Phys. Rev. B 36, (1987) 5719.

[8] J.D. Jorgensen, M.A. Geno, D.G. Hinks, L. Soderholm, K.J. Volin, R.L. Hitterman, J.D. Grace, I.K. Schuller, C.U. Segre, K. Zhang, and M.S. Kleefisch, Phys. Rev. B, 36, (1987) 3608.

[9] G. Van Tendeloo and S. Amelinckx, J. Electron Microsc. Tech., 8, (1988) 285.

[10] J.C. Barry, J. Electron Microsc. Tech., 8, (1988) 325.

[11] M. Sugiyama, R. Suyama, T. Inuzuka, and H. Kubo, Jpn. J. Appl. Phys., 26, (1987) L1202.

[12] T.E. Mitchell, T. Roy, R.B. Schwarz, J.F. Smith, and D. Wohlleben, J. Electron Microsc. Tech., 8, (1988) 317.

[13] D. de Fontaine, L.T. Wille and S.C. Moss, Phys. Rev. B, 36, (1987) 5709.

[14] G. Van Tendeloo, H.W. Zandbergen and S. Amelinckx, Solid State Comm., 63, (1987) 603.

[15] S. Iijima, T. Ichihashi, Y. Kubo, and J. Tabuchi, Jpn. J. Appl. Phys., 26, (1987) L1478.

[16] C.H. Chen, D.J. Werder, L.F. Schneemeyer, P.K. Gallagher, and J.V. Waszczak, Phys. Rev. B, 38, (1988) 2888.

[17] C.J. Jou, R. Kilaas, and J. Washburn, Lawrence Berkeley Laboratory Report, LBL-25149.

[18] C.S. Pande, A.K. Singh, L. Toth, D.U. Gubser, and S. Wolf, Phys. Rev. B, 36, (1987) 5669.

[19] H. Verweij, Solid State Comm., 64, (1987) 1213.

[20] D.C. Johnson, A.J. Jacobson, J.M. Newsam, J.T. Lewandowski, D.P. Goshorn, D. Xie, and W.B. Yelon, in "Chemistry of High-Temperature Superconductors," ACS Sym. Ser. 351, American Chemical Society, Washington, D.C., (1987) p. 148.

[21] J.Y. Henry, P. Burlet, A. Bourret, G. Roult, P. Bacher, M.J.G.M. Jurgens, and J. Rossat-Mignod, Solid State Comm., 64, (1987) 1037.

[22] K. Kishio, J.-I. Shimoyama, T. Hasegawa, K. Kitazawa, and K. Fueki, Jpn. J. Appl. Phys., 26, (1987) L1228.

[23] B.G. Hyde, J.G. Thompson, R.L. Withers, J.G. Fitzgerald, A.M. Stewat, D.J.M. Bevan, J.S. Anderson, J. Bitmead, and M.S. Paterson, Nature, 327, (1987) 402.

[24] H. Oyanagi, H. Ihara, T. Matsubara, T. Matsushita, M. Hirabayashi, M. Tokumoto, K. Murata, N. Terada, K. Senzaki, T. Yao, H. Iwasaki, and Y. Kimura, Jpn. J. Appl. Phys., 26, (1987) L1233.

[25] B. Raveau, C. Michel, and M. Hervieu, in "Chemistry of High Temperature Superconductors," ACS Sym. Ser. 351, American Chemical Society, Washington, D.C., (1987) p. 128.

[26] M. Hervieu, B. Domenges, C. Michel, and B. Raveau, Europhysics Lett., 4, (1987) 205.

[27] W.I.F. David, W.T.A. Harrison, J.M.F. Gunn, O. Moze, A.K. Soper, P. Day, J.D. Jorgensen, D.G. Hinks, M.A. Beno, L. Soderholm, D.W. Capone, I.K. Schuller, C.U. Segre, K. Zhang, and J.D. Grace, Nature, 327, (1987) 310.

[28] J.M. Tarascon, P. Barboux, B.G. Bagley, L.H. Greene, W.R. McKinnon, and G.W. Hull, in "Chemistry of High-Temperature Superconductors," ACS Sym. Ser. 351, American Chemical Society, Washington, D.C., (1987) p. 198.

[29] D.J. Werder, C.H. Chen, R.J. Cava, and B. Batlogg, Phys. Rev. B, 37, (1988) 2317.

[30] K. Hiraga, D. Shindo, M. Hirabayashi, M. Kikuchi, and Y. Syono, J. Electron Microsc. 36, (1987) 261.

[31] G. Van Tendeloo, H.W. Zandbergen, and S. Amelinckx, Solid State Comm. 63, (1987) 389.

[32] Y. Hirotsu, Y. Nakamura, Y. Murata, S. Nagakura, T. Nishihara, and M. Takata, Jpn. J. Appl. Phys. 26, (1987) L1168.

[33] G. Deutscher and K.A. Müller, Phys. Rev. Lett. 59, (1987) 1745.

[34] T.K. Worthington, W.J. Gallagher, and T.R. Dinger, Phys. Rev. Lett. 59, (1987) 1160.

[35] P.G. de Gennes, "Superconductivity of Metals and Alloys," Benjamin, New York, (1966) p. 229.

[36] N. McN. Alford et al., Nature 332, (1988) 58.

[37] A.G. Khachaturyan and J.W. Morris, Jr., Phys. Rev. Lett. 59, (1987) 2776.

[38] C.J. Jou and J. Washburn, Lawrence Berkeley Laboratory report, LBL-26065.

[39] C.J. Jou, E.R. Weber, J. Washburn, and W.A. Soffa, Appl. Phys. Lett. 52, (1988) 326.

[40] A. Ourmazd, J.A. Rentschler, W.J. Skocpol, and D.W. Johnson, Jr., Phys. Rev. B 36, (1987) 8914.

[41] P.G. de Gennes, "Superconductivity of Metals and Alloys," Benjamin, New York, (1966) p. 56.

[42] P. Norling, P. Svedindh, P. Nordblad, L. Lundgren, and P. Przyslupsky, Physica C, 153, (1988) 314.

[43] J.R. Fraser, T.R. Finlayson, T.F. Smith, G.N. Heintze, R. McPherson, and H.J. Whitfield, MRS Spring Meeting, Reno, Nevada, April 5–9, 1988 (in press).

[44] T.R. Finlayson, J.R. Fraser, T.F. Smith, R.H. Mair, G.N. Heintze, and R. McPherson, Australian Bicentenary Congress of Physicists, Sydney, January 25–29, 1988 (in press).

[45] F.M. Mueller, S.P. Chen, M.L. Prueitt, J.R. Smith, J.L. Smith, and D. Wohlleben, Phys. Rev. B 37, (1988) 5837.

LAWRENCE BERKELEY LABORATORY
CENTER FOR ADVANCED MATERIALS
1 CYCLOTRON ROAD
BERKELEY, CALIFORNIA 94720